Journal of Marine Systems 177 (2018) 53–61

Contents lists available at ScienceDirect

Journal of Marine Systems

journal homepage: www.elsevier.com/locate/jmarsys

Deposition and benthic mineralization of organic carbon: A seasonal study from Faroe Islands

Gunnvør á Norði [a,*,1], Ronnie N. Glud [b,c,d,e], Knud Simonsen [f], Eilif Gaard [a]

[a] Faroe Marine Research Institute, 100 Tórshavn, Faroe Islands
[b] University of Southern Denmark, Department of Biology, Nordic Center for Earth Evolution (NordCEE), Odense M, Denmark
[c] Greenland Climate Research Center (GCRC), Greenland Institute of Natural Resources, 3900 Nuuk, Greenland
[d] Scottish Association for Marine Science (SAMS), Scottish Marine Institute, Oban PA37 1QA, UK
[e] Artic Research Centre, Aarus University, 8000 Aarhus, Denmark
[f] Fiskaaling-Aquaculture Research Station of the Faroes, 430 Hvalvík, Faroe Islands

ARTICLE INFO

Article history:
Received 29 February 2016
Received in revised form 26 August 2016
Accepted 13 September 2016
Available online 14 September 2016

Keywords:
Sedimentation
Organic carbon
Lateral advection
Resuspension
Mineralization
Burial
Fjord

ABSTRACT

Seasonal variations in sedimentation and benthic mineralization of organic carbon (OC) were investigated in a Faroese fjord. Deposited particulate organic carbon (POC) was mainly of marine origin, with terrestrial material only accounting for <1%. On an annual basis the POC export from the euphotic zone amounted to 10.2 mol C m^{-2} yr^{-1} equating to 37% of the net primary production, and maximum sedimentation rates were associated to the spring bloom. The dynamics in the benthic solute exchange were governed by stratification that isolated the bottom water during summer and intensified sediment resuspension during winter. The POC export from the euphotic zone could not sustain the benthic mineralization rate (10.8 mol C m^{-2} yr^{-1}) and the calculated burial rate (9.8 mol C m^{-2} yr^{-1}) of organic material in the central basin. This indicated considerable focusing of material in the central part of the fjord. This was supported by the fact that the measured benthic mineralization rate – in contrast to most investigations – actually increased with increasing water depth. In August, when mineralization was at its maximum, the dissolved inorganic carbon (DIC) release from the sediment increased by 2.2 mmol m^{-2} d^{-1} for every m increase in water depth at 30–60 m depth. Due to sediment focusing, the OC burial in the deepest part of the fjord was 9.8 mol C m^{-2} yr^{-1}. This was 2.4 times higher than the average OC burial in the fjord, estimated from the total sedimentation, and benthic mineralization accounting for the water depth related changes in activity. The study in Kaldbaksfjørður underscore that fjords are important sites for long time OC burial, but emphasize the need for accounting for spatial variations when extrapolating results from a single or few stations to the scale of the entire fjord.
Regional terms: Faroe Islands, Kaldbaksfjørður

1. Introduction

Fjords are hotspots for deposition, mineralization and preservation of organic carbon (OC), and are estimated to account for 11% of the global long-term marine OC burial although they cover <0.1% of the global ocean surface area (Smith et al., 2015). However, carbon burial rates vary more than ten fold among fjords, reflecting the diversity in productivity and key drivers governing the preservation efficiency, such as the OC amount of terrestrial origin, or entrained from the marine environment outside the fjord (Sørensen et al., 2015; Wiedmann et al., 2015). The boundaries for OC production and consumption in the fjords also play a crucial role in preservation efficiency (Burdige, 2007). These boundaries represent the hydrographic settings governed by freshwater runoff from land as well as wind and tidal mixing, the nutrient and light availability, and the timing and abundance of biota consuming the OC produced (Skei et al., 2003).

The influence from anthropogenic activity remains one important factor that also is variable. In distinct unpopulated areas climate change is the main cause for long-term changes (Rysgaard et al., 1998; Sørensen et al., 2015; Wiedmann et al., 2015), while eutrophication can alter the carbon cycle significantly in fjords near densely populated and industrial areas (Lomstein et al., 1998; Therkildsen et al., 1993). Faroese fjords may be subjected to both influences. Eutrophication mainly from the expanding aquaculture and climate change, where the expected changes are warming and increased precipitation that may result in landslides (Hansen, 2011).

* Corresponding author.
E-mail addresses: gunnvor@fiskaaling.fo (G. á Norði), rnglud@biology.sdu.dk (R.N. Glud), knud@fiskaaling.fo (K. Simonsen), eilifg@hav.fo (E. Gaard).
[1] Current address: Fiskaaling-Aquaculture Research Station of the Faroes, 430 Hvalvík, Faroe Islands.

http://dx.doi.org/10.1016/j.jmarsys.2016.09.005
0924-7963/

In Faroese fjords, the persistent influence of the North Atlantic Current (Hansen and Østerhus, 2000) implies little seasonal variation in seawater temperatures (6–11 °C) and salinity (32–35.5) (Gaard et al., 2011). They do, however, exhibit seasonal variations in productivity due to variations in light availability, with day lengths from 5 h during winter to 20 h in the summer. Short-term variations in weather conditions can have major implications for the hydrography and productivity in Faroese fjords. Low pressures passing across the islands mainly from west induce strong wind events (>15 m s^{-1}) and heavy rain during all times of the year although more frequent during winter. These short-term fluctuations influence horizontal flow and vertical mixing of seawater in the fjords, which imply high nutrient availability in the euphotic zone. Thus, solar radiation rather than nutrient availability set the limit for primary production, which is 2–3 times higher production than in neighbouring regions, such as Icelandic, Norwegian and Scottish fjords (Gaard et al., 2011).

In this study, the seasonal variations in benthic supply and mineralization of organic material were investigated in a fjord that is located centrally in the Faroe Islands, representing settings sheltered from ocean swells and strong currents. Data are used to evaluate implication of spatial and temporal variations and to establish an annual carbon budget for the fjord.

2. Materials and methods

2.1. Study site and sampling scheme

The Faroe Islands is an archipelago, located at 62° N, 7° W. Kaldbaksfjørður is a classic long (6.6 km) and narrow (0.5–1.7 km) sheltered fjord. At the entrance is a sill at 40 m depth, while the maximum water depth is 60 m (Fig. 1). The general hydrography reflects a year round two-layered system. The 8–20 m deep surface layer (salinity: 32.1–34.9 and temperature: 5.8–11.4 °C) receives freshwater run-off from the 42 km^2 watershed through plentiful rivers distributed around the fjord, while the inflowing deep water mass (salinity: 34.9–35.3 and temperature: 6.2–10.8 °C) consists of Faroe Shelf water (Gaard et al., 2011). Wind induced mixing of the water masses occurs at all times of the year, creating a highly dynamic system, and a wide transition zone between the upper and lower water masses, rather than a sharp pycnocline. The density difference between the surface water and the deeper water is mainly due to salinity difference. During the study, the maximum density difference (1.55 kg m^{-3}) was observed in autumn, when precipitation was highest. Throughout the rest of the study, the stratification was weak, with density differences <0.5 kg m^{-3} (Gaard et al., 2011). From mid-June to September 2006, the water column was divided into 3 layers, due to an additional thermocline at ~40 m depth. The stratification led to isolated bottom water during this period and the O_2 concentration declined to a minimum of 136 μM in August (á Norði et al., 2011). The hydrodynamics cause a high flushing rate of the euphotic zone, with high inflow of nutrients throughout the summer. The season with sufficient light for primary production in the euphotic zone extends from April to October. These natural settings resulted in an annual primary production of ~335 g C m^{-2} yr^{-1} (Gaard et al., 2011).

The watershed of the fjord is mostly uncultivated and unpopulated. The main anthropogenic nutrient input to the euphotic zone was from fish farming activity. However, the high natural inflow of nutrients implies that the anthropogenic input has little effect on, the primary production (Gaard et al., 2011). Deposition of food and faecal waste from the fish farm had no effect on the overall conditions in the central basin targeted in this study (á Norði et al., 2011).

From May 2006 to May 2007, three sediment cores were on 11 occasions recovered at the 52 m deep station T (Fig. 1). The sediment cores were used to determine the inventory of OC and the benthic solute exchange of O_2, Dissolved inorganic Carbon (DIC), NH_4^+ and NO_3^-. At one occasion (October 2006) 12 sediment cores were sampled at 50–55 m bottom depth within an area of 1 km^2 near station T to evaluate potential spatial variation in the study area.

In August 2006 and 2007 sediment was sampled at 8 other locations covering a depth range of 35 to 55 m to evaluate any potential depth relation in diagenetic activity. In October 2009 sediment cores were taken for determination of excess ^{210}Pb to assess the carbon burial rate at station T.

Vertical particle and OC fluxes were continuously measured with sedimentation traps deployed at 20, 40 and 50 m depth near station T. In addition, the C:N ratio of the suspended material was measured at 5, 10 and 20 m depth in the water column on 11 occasions throughout the study period. The carbon content and C:N ratio of riverine material was measured in three of the rivers entering the inner part of the fjord in January and February 2009 (Fig. 1).

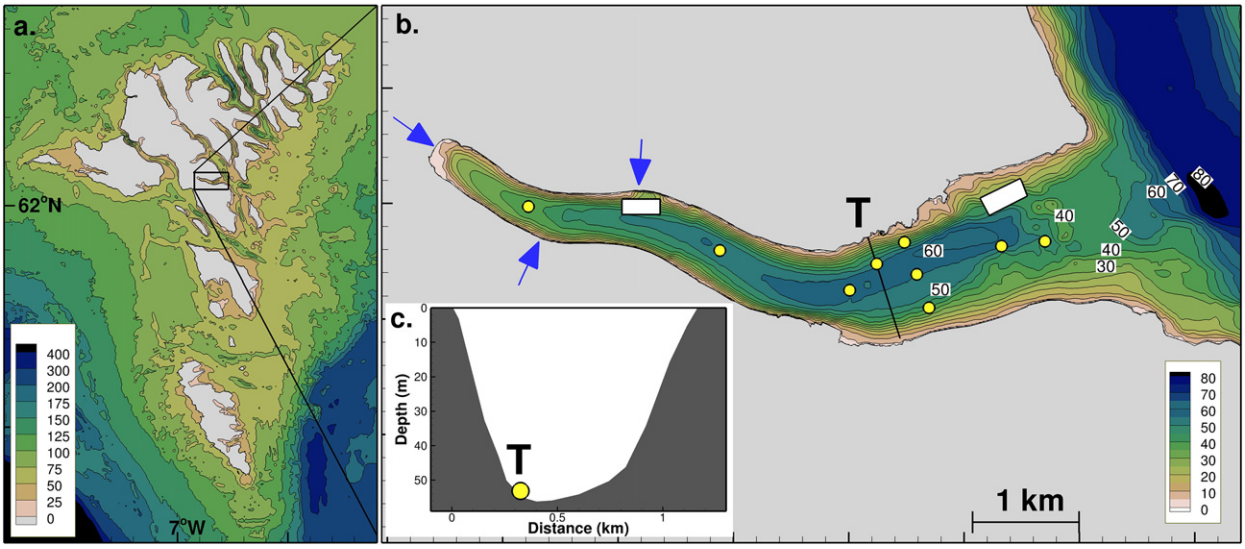

Fig. 1. (a) location of Kaldbaksfjørður in the central Faroe Islands (b) Sediment sampling stations (yellow dots). The time series sampling station is marked T. Blue arrows mark the rivers, where OC and C:N ratio in riverine water was measured. The two fish farming areas in Kaldbaksfjørður are shown as white blocks, but they did not affect conditions at the measuring sites. (c) Bottom depth at a north-south cross section (indicated by a black line in (b)) through station T which is located at the base of the ~14° steep slope.

2.2. Sedimentation

Duplicate sedimentation traps (Ø 110 mm, length 700 mm, KC-Denmark) were moored at 20, 40 and 50 m depth near station T. The traps were replaced every 2–3 weeks, with exception of the deployment in February - Mars 2007 which lasted 40 days. At each depth, one trap was kept unpreserved while the other was preserved with a poisonous solution of formaldehyde (4%) added to dense seawater (salinity ~60). After trap recovery, sub-samples of the content were filtered on pre-combusted (475 °C) and pre-weighed Whatman GF/F filters. In order to remove dissolved organic carbon and nitrogen, the filters were flushed with artificial seawater. The flux of total particulate material (TPM) was determined by the weight gain of the filters after drying at 60 °C. Particulate organic carbon (POC) and nitrogen content, as % of dry weight, was determined from sub-samples of the dried filters, which were fumed with concentrated HCl for 16 h to remove any potential contribution from inorganic carbon, prior to analysis on a CE 440 Elemental analyser.

The difference between the preserved and unpreserved traps was highest at 20 m depth, where the averaged carbon flux was 1.4 ± 0.22 times ($n = 17$) higher in the preserved trap compared to the unpreserved trap. At 40 m depth the average ratio was 1.3 ± 0.08 while no difference was observed at 50 m depth. The C:N ratio was lower in the preserved trap compared to the unpreserved, and as for the carbon content the difference was highest in the most shallow trap. Therefore, we decided only to apply data from preserved traps as these were considered most trustworthy (see Section 4.1).

The carbon and nitrogen content in riverine particulate matter and in seawater at 5, 10 and 20 m depth was measured by filtrating 0.5 L of riverine water or 1 L of seawater through precombusted Whatman GF/F filters and quantification was performed as described above.

2.3. Sediment characteristics

Sediment was retrieved with a HAPS bottom corer (Kanneworf and Nicolaisen, 1973). Only cores with a clear overlying water phase were used. For further analysis, sub-cores were collected in plexiglas liners (i. d. 5.6 cm) which were kept in darkness and at bottom water temperature during the 4 h transport time to the laboratory.

Total OC and nitrogen content was measured in the uppermost cm of the sediment by a CE 440 Elemental analyser after the sediment had been homogenized, acidified (4–5% H_2SO_4) in order to remove inorganic carbon, and dried. Sediment porosity was determined from the measured density and water content measured as the weight loss after drying at 70 °C for ~48 h.

For measurements of excess ^{210}Pb, sediment cores were sliced into 0.5 cm intervals down to 5 cm and 1 cm intervals down to 15 cm. The samples for excess ^{210}Pb measurements were dried and ground before 10–15 g of sediment was packed into polyethylene containers, sealed, and left to condition for at least two months prior to counting. The activity of ^{210}Pb and ^{226}Ra were determined by gamma spectroscopy using high-purity germanium detectors. Excess ^{210}Pb was taken as the difference between total ^{210}Pb activity and the activity of ^{226}Ra. The sediment accumulation velocity (w) was calculated from the exponential decrease in excess ^{210}Pb activity, below the zone affected by bioturbation (~4.5 cm), assuming an uniform initial background concentration of ^{210}Pb (Appleby and Oldfield, 1992). The sediment burial rate $F_{sed} = w(1 - \varphi)\rho$ was calculated from the sediment accumulation velocity, the porosity (φ) and the density (ρ) of the sediment. The OC burial rate $F_{OC} = (1 - \varphi)\rho OC$ was estimated using average measured value of OC from the depth interval of 15–20 cm.

2.3.1. Benthic solute exchange rates

The total oxygen uptake (TOU) and efflux of DIC from the sediment, as well as the exchange rates of NO_3^- and NH_4^+, were measured by whole core incubations. Three sediment cores were submerged in an incubation tank, holding bottom water at in situ temperature ± 0.5 °C. On most sediment sampling dates the bottom water was >90% air-saturated and the incubation tank was air flushed, keeping the difference between the in situ and tank oxygen concentration below 30 μM. However, in August 2006 when the in situ O_2 content in the isolated bottom water only had 48% air saturation, the incubation tank was flushed with a mixture of nitrogen and air, which kept the saturation at 60%, thus 33 μM higher oxygen concentration than the in situ conditions. The remaining flux measurements conducted in August 2006 and 2007 were on sediment sampled at stations unaffected by O_2 depletion, and cores were therefore incubated in air saturated bottom water. The higher O_2 concentration in the incubation tank on a few sampling days might have increased the O_2 consumptions rate slightly as compared to natural settings. In order to ensure well mixed conditions of the overlying water, small rotating Teflon-coated magnets were attached to the inner wall of the core liners. The magnets received momentum from an externally rotating magnet (Rasmussen and Jorgensen, 1992).

After pre-incubation (12–24 h) the cores were closed, leaving an internal water height of approximately 8 cm. Oxygen concentration in the cores was monitored with a Clark type oxygen minielectrode with an external tip diameter of 500 μm, 90% response time of ~2 s and stirring sensitivity of <1% (Gundersen et al., 1998; Revsbech, 1989). Samples for measurements of O_2, DIC, NO_3^- and NH_4^+ content were taken at the start of the incubation and when the O_2 concentration inside the cores had decreased by 15–20% of the initial value as monitored by the electrode. The samples were collected with a glass syringe equipped with a Tygon tube. For O_2 and DIC concentration measurements, the water was transferred to 12 mL and 1.5 mL gas tight glass vials, respectively. Oxygen concentration was determined by Winkler titration (Grasshoff et al., 1999), while DIC samples were preserved with 20 μL of $HgCl_2$ (5% w/v) until later analysis on an infrared gas analyser (ADC-225-MK3). NO_3^- and NH_4^+ samples were collected in 20 mL plastic vials, filtered through GFC filters and preserved with 3 droplets of chloroform. NO_3^- was measured on an autoanalyser according to Grasshoff et al. (1999) and NH_4^+ was measured manually by the salicylate-hypochlorite method (Bower and Holm-Hansen, 1980).

Sediment-water fluxes were calculated assuming linear concentration changes of the respective solutes during incubation, and by accounting for the incubation time and the enclosed water volume. A linear decline in the O_2 concentration was confirmed by the continuous recording of the electrode, and similar investigations have shown the concentration of the other solutes to decrease linearly when the change in oxygen concentration is <20% as in this study (Brenner et al., 2016; Glud et al., 1998, 2016). The monthly measurements were integrated to annual rates by linear extrapolation between the respective measuring dates, and an annual molar respiration quotient (RQ; mol DIC/mol TOU) calculated. TOU is frequently used as a proxy for total carbon mineralization under the assumption of a fixed RQ, usually in the range of 1–1.2 (Carlsson et al., 2012; Glud, 2008; Jørgensen et al., 2005).

2.3.2. Oxygen microprofiles

Oxygen microprofiles were measured in the same sediment cores 12 h after the flux measurements had been terminated by cap removal. Profiles were obtained with a Clark-type microelectrode with the same measuring characteristics as listed above, but with a tip diameter of only ~10 μm. Three profiles were measured in each core. The microelectrode was positioned with a motor driven micromanipulator and profiles were measured at a depth resolution of 100 μm. The sensor current was measured by a picoammeter connected to an A/D converter, which transferred the signal to a PC (Revsbech and Jørgensen, 1986). The microelectrode was calibrated by two-point calibration from the signal in the overlying water of known O_2 concentration and the signal in deep anoxic sediment layers.

Oxygen penetration depth (OPD) was obtained from the oxygen microprofiles, as the depth between the sediment surface and the onset of the constant anoxic signal. The position of the sediment surface

was estimated from a shift in the otherwise linear concentration gradient throughout the diffusive boundary layer of the individual profiles (Glud et al., 1995). The diffusive oxygen uptake (DOU) was calculated from the summarized volume specific oxygen consumption in the sediment, estimated from the oxygen microprofiles by the software PROFILE (Berg et al., 1998). The difference between TOU and DOU mainly reflects fauna related O_2 consumption including irrigation and respiration (Glud et al., 2003).

3. Results

3.1. Sedimentation

The vertical POC flux at 20 m depth, which represented the lower limit of the euphotic zone, showed a distinct seasonal signal, with highest export rates of 91 and 83 mmol C m^{-2} d^{-1} in May 2006 and 2007, respectively (Fig. 2). The POC export decreased during summer, and was at its minimum from late September to April where it ranged between 17 and 23 mmol C m^{-2} d^{-1}. The annual POC export amounted to 13.8 mol C m^{-2} and the concurrent PN export was 1.8 mmol N m^{-2} yr^{-1}. 1. The productive period (April – September) – as previously identified by Gaard et al. (2011) accounted for 75% and 84% of the total annual POC and PN, respectively.

The molar C:N ratio of the sinking particulate material varied greatly during spring and summer 2006 (5.7–8.6), with the highest ratio during the period with maximum sedimentation (Fig. 2). The value for suspended matter was stable with C:N ratios between 6.2 and 6.5 during spring increasing to a range of 6.9 and 7.6 during summer. The highest molar C:N ratio of 9.6 in the suspended matter was observed in November (Fig. 2). In January and February 2009, the C:N ratio of material entering the fjord from three of the rivers, varied greatly among rivers (Table 1), but the mean ratio was lower than the ratio of the material caught in the sediment traps.

The vertical flux of total particular matter (TPM) at 20 m depth showed no seasonal trend (Fig. 2). However, the flux increased with depth, especially from autumn to spring. Vertical POC fluxes likewise increased with depth (Fig. 2). For instance, the POC flux at 50 m depth was 1.1 ± 0.04 times the flux measured at 20 m from May to August, but from September to April the flux at 50 m depth was 3 times higher than the flux at 20 m depth. The gradually increase in TPM and POC sedimentation with increasing water depth presumably reflect resuspension of material that enters the lower traps, particularly during the more energetic periods of the winter season.

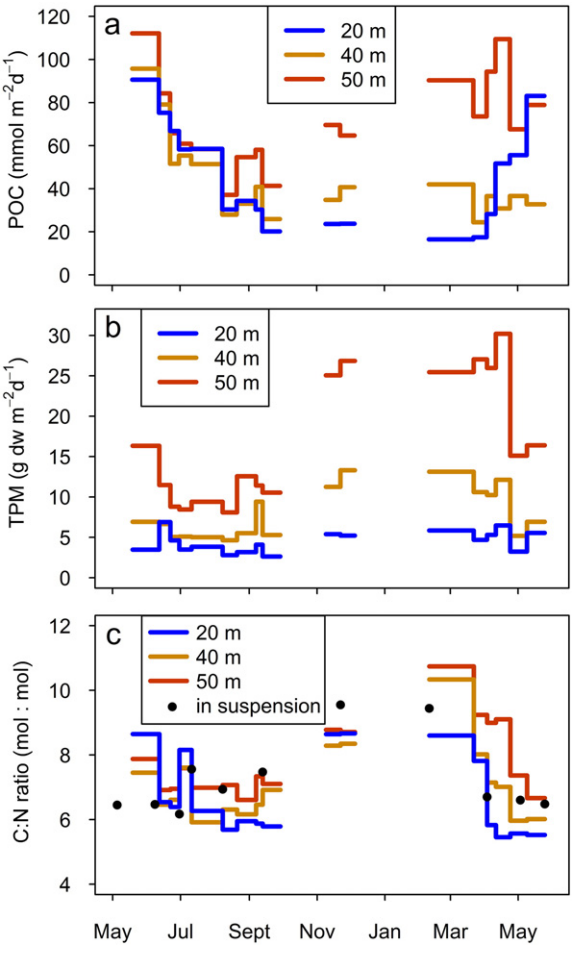

Fig. 2. Seasonal variations in vertical fluxes of (a) particulate organic carbon and (b) total particulate matter at 20, 40 and 50 m depth in the water column. (c) C:N ratio of the sinking particles (lines) and average C:N ratio of particles in suspension at 5, 10 and 20 m depth in the water column (dots). Width of intervals represents sedimentation trap deployment time. The C:N ratio and POC content in settling particles at 20 m have formerly been published as a reference station in á Norði et al. (2011).

3.2. Seasonal variation in the sediment

The bottom water temperature changed annually between 6.2 and 10.8 °C, with maximum and minimum temperatures in late September and March, respectively (Fig. 3a). The O_2 concentration in the bottom water was close to air saturation at most sampling dates, but from June a transient thermocline at ~40 m depth (Gaard et al., 2011) caused the O_2 concentration in the bottom water to decline (Fig. 3b). Minimum O_2 concentration of 136 μmol L^{-1} was measured in August, but in late September the O_2 level of the bottom water was again close to air saturation. The OPD ranged from a minimum of 1.1 mm when the O_2 availability in the water column was at its minimum, to the maximum of 4.4 mm in March (Fig. 3c). The TOU of the sediment ranged from 13 ± 1 mmol m^{-2} d^{-1} during winter to a peak of 51 ± 13 mmol m^{-2} d^{-1} just after the apparent renewal of the bottom water in September (Fig. 3d). The seasonal changes in DOU were less pronounced, ranging between 5.6 and 14 mmol m^{-2} d^{-1}. The integrated annual DOU amounted to 39% of TOU, with higher contribution during summer than winter, indicating that benthic fauna was more important for the TOU during summer. The annual TOU was 8.4 mol m^{-2}.

In contrast to TOU, which was relative constant during spring and summer 2006, the DIC efflux gradually increased and reached its maximum in the period with maximum bottom water temperature in August and September (Fig. 3e). Overall, the DIC efflux exhibited a considerably higher seasonal variability than TOU and ranged between 3.5 ± 2.3 and 79.1 ± 7.5 mmol m^{-2} d^{-1}. Correspondingly the respiratory quotient varied with a summer maximum of 2.8 ± 0.5 and a winter minimum of 0.3 ± 0.1 during December (Fig. 3e). The annual DIC exchange was 10.8 mol m^{-2}, thus the yearly integrated RQ amounted 1.3. Generally, there was a net NH_4^+ efflux from the sediment (Fig. 3f) and typically high rates coincided with low O_2 availability in the sediment. On the few occasions, the net NH_4^+ exchange was a sediment uptake the fluxes were small >0.03 mmol m^{-2} d^{-1}.

To evaluate the spatial variation in solute exchange around station T, sediment cores were retrieved at 12 locations within a 1 km^2 area of station T, and fluxes of TOU, NH_4^+ and NO_3^- were measured individually.

Table 1
Mean organic carbon content and molar C:N ratio ± (SE) in three of the rivers entering Kaldbaksfjørður measured on two sampling dates in 2009. The range in daily precipitation three days prior to the measurement is also shown (precipitation data from www.dmi.dk).

Date	Organic carbon (mmol m^{-3})	C:N ratio (mol:mol)	Precipitation (mm d^{-1})
26 January	7.9 ± 3.4	8.1 ± 1.3	2–7
16 February	15.0 ± 4.4	7.9 ± 0.8	4–14

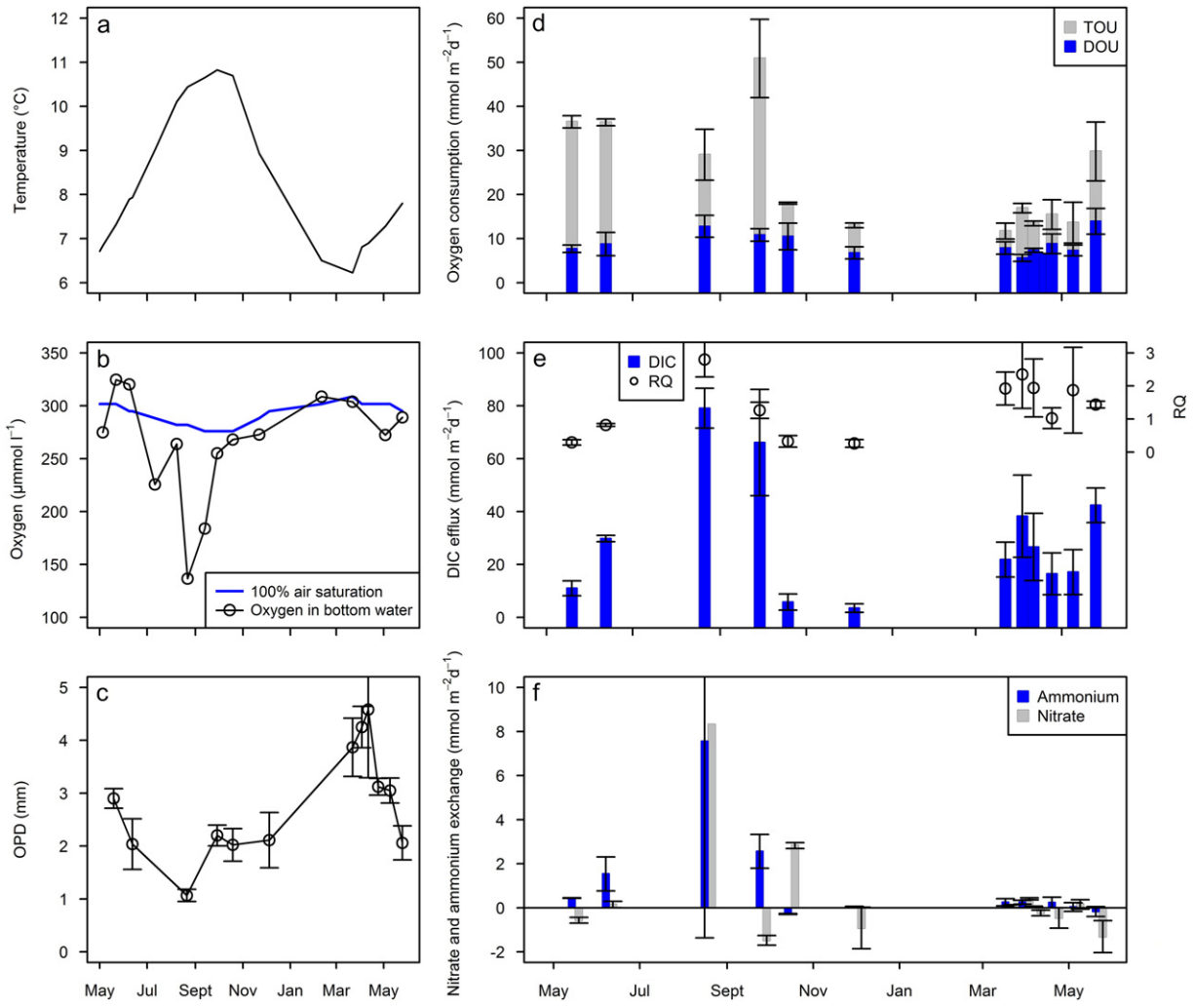

Fig. 3. Seasonal variation in (a) sea water temperature at 40 m depth, (b) oxygen concentration at 50 m depth and at 100% air saturation (blue line). (c) Oxygen penetration depth (OPD) (d) the total (TOU) and diffusive (DOU) oxygen uptake of the sediment (e) efflux of dissolved inorganic carbon (DIC) and the respiratory quotient (RQ) (f) exchange rates of ammonium and nitrate. Negative values represent sediment uptake. Error bars indicate SE, n = 9 for DOU and OPD and 3 for the solute exchange rates. Data on bottom water temperature are from Gaard et al. (2011) and data on the bottom water oxygen concentration are from á Norði et al. (2011).

The range in TOU was 18.5 mmol m^{-2} d^{-1}–33.9 mmol m^{-2} d^{-1}, NH_4^+ ranged from −0.48 mmol m^{-2} d^{-1} to 2.43 mmol m^{-2} d^{-1}, while the range in NO_3^- was −0.6 mmol m^{-2} d^{-1} to −0.1 mmol m^{-2} d^{-1}.

To assess the contribution of spatial variations to the measured rates we combined the measured exchange rates into every possible mean of 2 and 3 at the locations (Fig. 4). The variations in obtained mean values

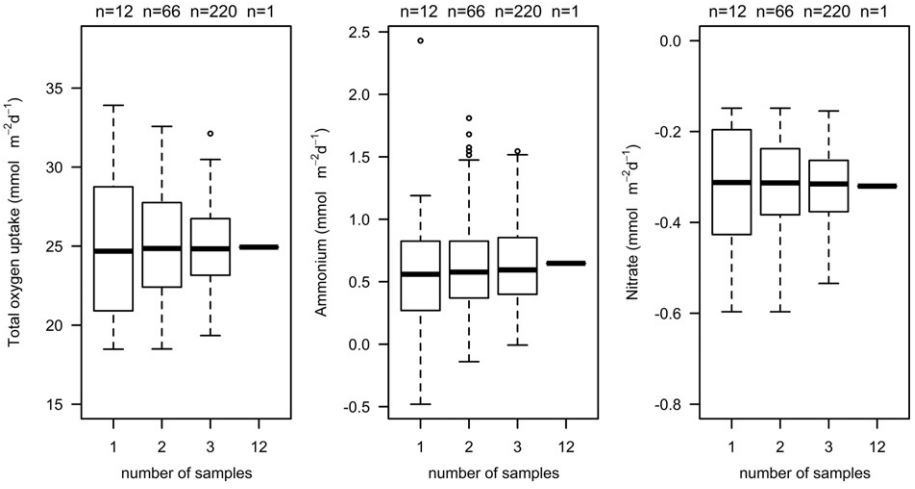

Fig. 4. Boxplots of mean values for every plausible combination of 1, 2 or 3 of the solute exchange rates in 12 sediment samples retrieved within 1 km^2 from station T in October 2009.

decreased with increasing number of averaged cores, with exception from the NH_4^+ flux, where an outlier affected the combination of means to a great extent (Fig. 4). By averaging 3 measurements, the obtained TOU rates were within 5 mmol m^{-2} d^{-1} from the mean value of 12 cores, with 50% of the TOU rates within 2 mmol m^{-2} d^{-1}. Thus the spatial variation was small compared to the seasonal change measured as a mean of 3 cores (Fig. 3). The spatial variation of nutrient exchange rates was likewise small compared to the seasonal changes. The 1 km^2 is more than ten times the size of the expected sampling area for seasonal measurements, as the vessel was attached to a permanent mooring during sampling, and thus the influence from spatial variation on the time series is expected to be smaller than the variation resolved in 1 km^2 area.

3.3. Carbon preservation in the sediment

The excess ^{210}Pb content decreased exponentially with depth below a ~4.5 cm deep surface zone with apparent mixing (Fig. 5). The bulk density and porosity changed rapidly in the uppermost part of the sediment, but was relatively constant at greater depth. The OC content decreased from 2.5% at the surface to an average of 2.2% at 15–20 cm depth. The C:N ratio increased from 8.0 at the surface to 8.7 at 15–20 cm depth. The calculated average sediment accumulation rate of 0.51 ± 0.04 cm yr^{-1}, corresponds to a sediment burial rate of 5381 ± 462 g m^{-2} yr^{-1}, which is 4.5 times the annual vertical flux of TPM at 20 m depth. Using the carbon content at 15–20 cm depth, where the OC content and C:N ratio were relatively constant, the OC burial was 118 ± 11 g C m^{-2} yr^{-1} (9.8 mol C m^{-2} yr^{-1}), which is similar to the annual carbon mineralization. Thus, calculated on area basis, the mineralization and burial rate of organic material exceeded the annual sedimentation rate by a factor of 1.5. This implies considerable focusing of material towards the targeted study site in the central part of the fjord.

3.4. Water depth related variations in the sediment

Sediment sampled at 8 locations covering the innermost to the outermost part of Kaldbaksfjørður (depth 35–55 m) consisted of a mixture of mud and clay in August. The OC content at 0–1 cm depth in sediment varied between 1.2 and 2.6%, and did not change significantly with water depth (Fig. 6). However, the C:N ratio decreased with increasing water depth. According to the linear model, the C:N ratio decreased from 8.7 at 35 m depth to 7.9 at 55 m depth. The solute exchange rates also changed as a function of water depth (Fig. 6). While the TOU for the three stations shallower than 41 m, were similar with an average of 22.4 ± 1.7 mmol m^{-2} d^{-1}, the value for the two deeper sites was 37.2 ± 3.3 mmol m^{-2} d^{-1}. Similarly, the DIC and NH_4^+ efflux appeared to increase with increasing water depth. Simple linear relation would project that the DIC efflux increased with 2.2 mmol m^{-2} d^{-1} for every m the depth increased, while the corresponding value for NH_4^+ was 0.089 mmol m^{-2} d^{-1}. The NO_3^- flux changed from a release from the sediment at the shallower stations to NO_3^- uptake at the deeper stations (Fig. 6). There was no pronounced inter annual variability in sediment characteristics, nor solute exchange rates. However, in 2006 solute exchange was only measured at the shallower stations, due to the low oxygen content in the isolated bottom in August 2006.

4. Discussion

4.1. Evaluation of the measured sedimentation rates

In this study, sedimentation of particulate matter was measured by long-term sedimentation trap deployments with formaldehyde as a preservant. Thus, poisoned swimmers actively seeking the traps might have increased the assessed vertical fluxes. Unpreserved traps, on the other hand, might be affected by grazing and microbial degradation (Buesseler et al., 2007). Influence from swimmers was indicated in some samples, where the C:N ratio was less than the average ratio of material in suspension (Fig. 2). It might be expected that the C:N ratio would decrease as a function of deployment time, due to the continuous stream of swimmers to the sedimentation traps. However, no correlation was found between duration of deployments (6–40 days) and the C:N ratio, or POC content of the traps. Thus, the influence was presumably small.

4.2. Seasonal variation in vertical fluxes

The POC export from the euphotic zone showed the typical seasonal pattern of fjords, with maximum export in association with the spring bloom, and a progressive decline during summer (Sørensen et al., 2015; Wassmann, 1984; Wiedmann et al., 2015). The C:N ratios of the sinking material resembled those of particles suspended in the upper 20 m of the water column, with ratios between 5.7 and 8.6 during spring and summer (Fig. 2). These are close to the Redfield ratio (6.6), thus the suspended and sinking material was mainly fresh material of marine

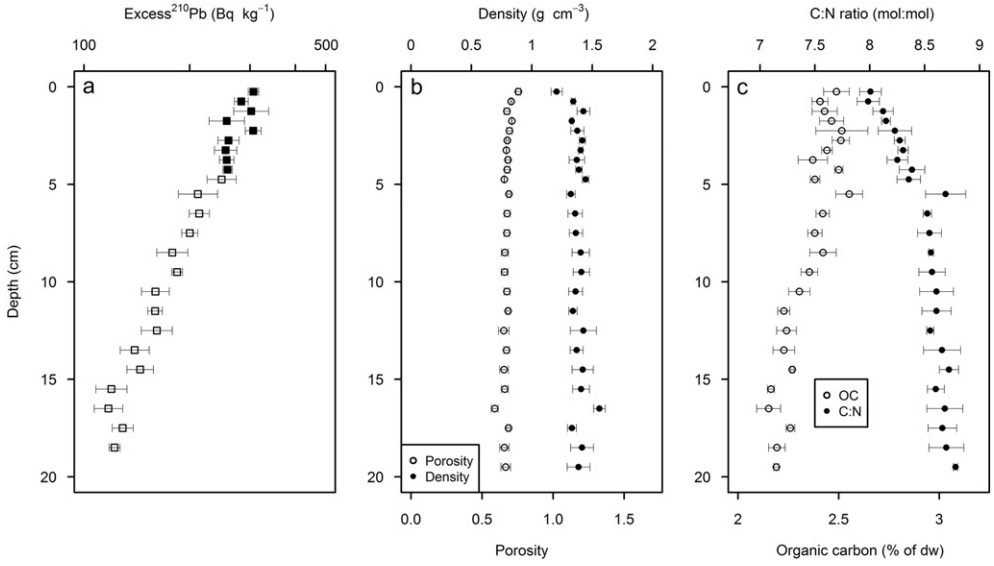

Fig. 5. Depth profiles of (a) excess ^{210}Pb, (b) porosity and bulk density and (c) organic carbon content and C:N ratio. Presented values are mean values (±SE) from three replicate sediment cores at station T in October 2009. Filled symbols in the left figure represent the surface zone affected by bioturbation, which is excluded from burial rate calculations.

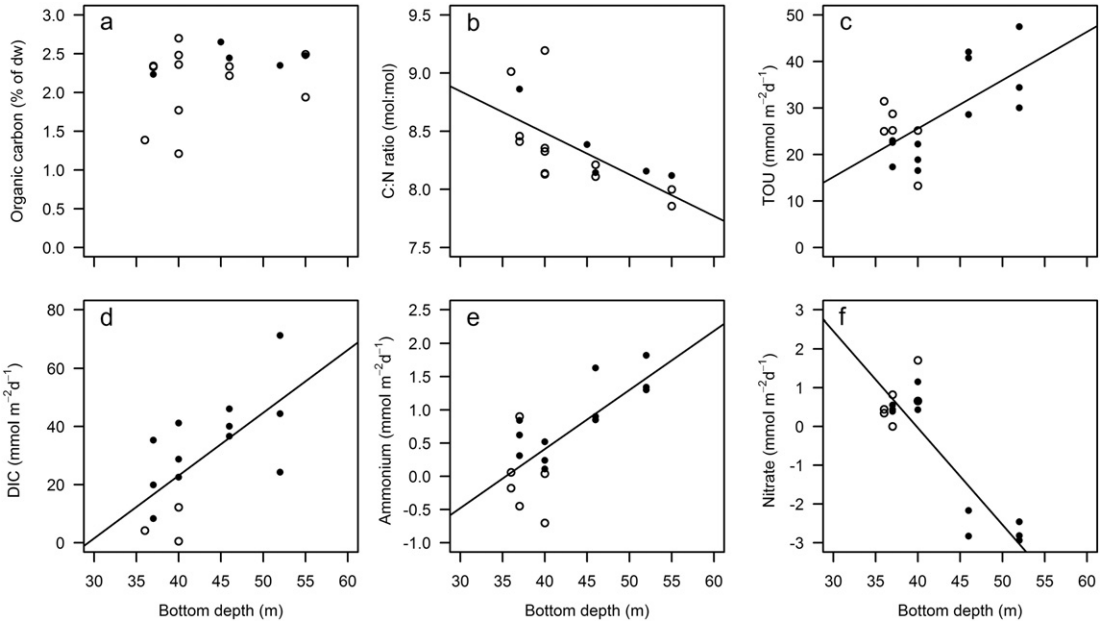

Fig. 6. Water depth related change at 30 to 60 m depth in (a) the OC content and (b) C:N ratio at 0–1 cm depth in the sediment. (c) TOU (d) dissolved inorganic carbon release and the exchange rate of (e) ammonium and (f) nitrate at 8 locations in Kaldbaksfjørður in August 2006 (open symbols) and August 2007 (filled symbols). Lines show the linear change in C:N ratio and fluxes as a function of depth. $C:N_{30\text{–}60\ m}$($Y = -0.036x + 9.9$, $F_{1,15} = 12.04$, $p < 0.01$), $TOU_{30\text{–}60\ m}$($Y = 1.04x - 16.1$, $F_{1,16} = 11.65$, $p < 0.01$), $DIC_{30\text{–}60\ m}$($Y = 2.16x - 63$, $F_{1,13} = 10.35$, $p < 0.01$), $NH_4^+{}_{30\text{–}60m}$($Y = 0.089x - 3.15$, $F_{1,16} = 18.4$, $p < 0.001$), NO_3^- ($Y = -0.25x + 10$, $F_{1,16} = 50.49$, $p \ll 0.001$). All cores were incubated in bottom water flushed with air.

origin (Lund-Hansen et al., 2004). During this period large sized diatoms of the genera *Coscinodiscus* sp. dominated the phytoplankton community while flagellates were more abundant in September (Gaard et al., 2011).

During winter the C:N ratio of the suspended matter was as high as 9.4–9.5 while it was 8.6–8.7 in the sinking material (Fig. 2). This is comparable to the C:N ratio in the sediment and that of particles suspended in riverine water (Table 1 and Fig. 6). The freshwater runoff from land was three times higher during winter than summer. From October to March the total long-term average runoff was 5.2 $m^3\ s^{-1}$ (Gaard et al., 2011). Applying the average POC content of riverine water (Table 1), the total OC supply from land during winter was 5140 mol OC d^{-1}. Evenly distributed in the fjord, it corresponds to a daily export of 0.95 mmol OC $m^{-2}\ d^{-1}$, which still only accounts for a minor fraction of the OC sedimentation during winter. In most fjords terrigenous OC contributes significantly more to the total OC sedimentation (Burdige, 2007; Smith et al., 2015; Wiedmann et al., 2015). However, the area of the watershed relative to the surface area of Kaldbaksfjørður is small and primary production high compared to other fjords.

Macroalgal detritus can sometimes contribute significantly to the OC pool accumulating in central basins of fjords and sounds (Fredriksen, 2003; Renaud et al., 2015). The macroalgal biomass and production in Kaldbaksfjørður is unknown. However, the steep shorelines together with high phytoplankton production which implies a high light attenuation coefficient (Gaard et al., 2011) limits the area where macroalgae can thrive, and thus their contribution to the total OC pool is expected to be small.

Sediment resuspension intensity increased during winter as observed from the increase in TPM and OC with depth (Fig. 2), and it is likely that the material with the higher C:N ratio in the upper 20 m in the water column was resuspended matter. Thus, the annual POC export from the euphotic zone of 13.8 mol $m^{-2}\ yr^{-1}$ most likely was overestimated, while the POC export from April to September (10.2 mol C m^{-2}) is a more accurate estimate of the annual POC export. 82% of the annual primary production occurred during this period (Gaard et al., 2011).

4.3. Seasonal variations in carbon mineralization

The benthic mineralization rates as inferred from the DIC efflux only poorly reflected variations in the sedimentation rates, as maximum mineralization coincided with the highest bottom water temperatures rather than highest POC export (Fig. 3). Despite the small seasonal variations in seawater temperature, variations in solute exchange rates were quite large. This might be expected under the given settings with high primary production and limited bottom water renewal during summer and intensified resuspension during winter.

The most pronounced seasonal signal was in the DIC efflux, which ranged from 3.5 mmol $m^{-2}\ d^{-1}$ to 79.1 mmol $m^{-2}\ d^{-1}$. The seasonal variations in TOU were not as distinct. The maximum DIC exchange occurred when the bottom water was isolated and the TOU limited by the reduced O_2 availability and mineralization was presumably dominated by anaerobic pathways like sulphate and iron reduction (Fig. 3). During winter the greater TOU than DIC efflux indicated continuous reoxidation of reduced metabolites like FeS and FeS_2 that had accumulated during the summer (Glud, 2008; Kristensen, 2000). The seasonal dynamics in TOU and DIC exchange resembles observations in the highly studied Aarhus bay (Glud et al., 2003; Thamdrup et al., 1994), where reduced oxygen content in the bottom water limited the oxygen supply to the sediment during periods of deposition of phytodetritus, and the accumulated reduced metabolites were subsequently reoxidized during the winter period. In Aarhus bay only 42% of the total annual carbon mineralization occurred under aerobic conditions (Glud et al., 2003). In general oxygen respiration accounts for half of the carbon mineralization in shallow coastal sediments (Canfield et al., 2005), and anaerobic pathways become increasingly important as the carbon supply increases or oxygen availability decreases (Glud et al., 2003; Jørgensen, 1996). Thus it is likely that at least half of the carbon mineralization at station T occurred under anaerobic conditions. But as an annual integral the TOU would still represented the sum of the aerobic and anaerobic mineralization processes.

While DIC efflux provides the best measure of the concurrent benthic mineralization rate, TOU integrates the activity on longer time scales by integrating aerobic respiration and reoxidation processes.

The annual integrated RQ of 1.3 could be interpreted as long time accumulation of reduced metabolites in the sediment, since RQ of 1–1.2 are common for mineralization of marine organic material (Carlsson et al., 2012; Glud, 2008; Jørgensen et al., 2005). However, such conclusions should be made with great caution as our measuring approach only poorly capture conditions during resuspension events, during which considerable reoxidation could take place (Porter et al., 2010).

The NH_4^+ efflux increased with decreasing OPD (Fig. 3). This probably reflects reduced nitrification, following reduced O_2 availability (Rysgaard et al., 1994).

The net nitrogen efflux ($NH_4^+ + NO_3^-$) from the sediment was very small compared to the DIC flux. The integrated yearly C:N ratio was 60, which suggests that only a small part of the mineralized nitrogen is reflected in the NH_4^+ and NO_3^- fluxes (Fig. 3), and could be indicative of high denitrification rates or efflux of dissolved organic nitrogen (Canfield et al., 2005), pathways which were unexplored in this study.

4.4. Water depth dependent variations in the sediment

The OC in the top of the sediment was within the range previously reported in fjords (Smith et al., 2015) and did not change with bottom depth (Fig. 6). However, the decreasing molar C:N ratio with increasing water depth, suggests that the organic material in the deepest part of the fjord was the least degraded in August. This is opposite to the general relation between OC quality in sediment and water depth (Arndt et al., 2013; Morata et al., 2008). The solute exchange also showed that the most labile OC was located at greatest water depth as the oxygen uptake and the release of inorganic carbon and ammonium increased with increasing depth (Fig. 6). In Kaldbaksfjørður resuspension occurred year round all though it was intensified during winter (Fig. 2). Resuspension presumably causes lateral advection and focusing of the sedimenting material towards the deepest part of the fjord – including redistribution of freshly deposited phyto-detritus during the productive periods of the year (Noji et al., 1993; Wassmann, 1984; Wiedmann et al., 2015). In contrast to most studies, the sediments in Kaldbaksfjørður therefore exhibited an inverted relation between OC turn-over and water depth.

4.5. Carbon cycling in Kaldbaksfjørður

Fjords are characterized by high rates of OC burial and contribute significantly to the worlds long term OC burial (Cui et al., 2016; Smith et al., 2015). Both the sediment burial rate of 5381 ± 462 g m^{-2} yr^{-1}, and OC burial of 118 ± 11 g C m^{-2} yr^{-1} at station T are in the higher end of reported values for burial rates in fjordic settings, which in turn show a substantial range. Sediment burial rates range 3 orders of magnitudes while OC burial rates varying more than tenfold (data compiled by Smith et al. (2015) and Cui et al. (2016)). The high burial rates at station T are similar to those in fjords located in Alaska, Svalbard and Greenland that are highly influenced by glacial meltwater (Gilbert et al., 1998; Sørensen et al., 2015; Walinsky et al., 2009; Zajączkowski et al., 2004). Even though the Faroe Islands have no glaciers, vast amounts of fresh water enter the fjord from the watershed (Gaard et al., 2011), and the characteristics of OC burial in Greenlandic and Alaskan fjords, with high contribution of carbon produced in primary production stimulated by nutrients supplied by entrained sea water (Cui et al., 2016) presumably also applies to Kaldbaksfjørður.

In general the fraction of total OC input to the sediment which escapes mineralization i.e. the burial efficiency (OC_{burial}/OC_{input}) increases with the sediment burial rate (Burdige, 2007; Canfield, 1994). The burial efficiency in the central area of the fjord was 48%, assuming that the OC burial and the benthic mineralization at station T equals the total OC deposition. This matches the empirical relation between sediment burial rates and carbon preservation as compiled by Canfield (1994).

Nevertheless, the steep topographies of fjords enhance sediment focusing towards the deepest areas causing the OC burial in the central fjord to be higher than in the shallow areas (Sugai, 1990). Thus the values derived at station T do not represent the fjord integral. However, the carbon burial in the fjord as a whole can be estimated from the total sedimentation and mineralization. Applying the trap data at 20 m water depth from April to September, the representative total POC annual input to the seabed in Kaldbaksfjørður was 4.94 · 10^7 mol OC yr^{-1} (Fig. 7). The total OC mineralization can be approximated (Fig. 7) from i) the bathymetry of the fjord, ii) the relation between water depth and DIC efflux (Fig. 6) and iii) the annual carbon mineralization rate at station T (Fig. 3), assuming a constant relation between mineralization rates and depth over the year. This gives a total annual carbon mineralization of 3.03 · 10^7 mol OC (Fig. 7). Thus, the burial efficiency for the fjord as a whole was ~39%, and the average OC burial rate as estimated from the OC sedimentation and burial efficiency was ~48 g C m^{-2} yr^{-1} (~4 mol C m^{-2} yr^{-1}). This is 2.4 times lower than the OC burial in the central basin, but still places Kaldbaksfjørður among fjords with high OC burial rates and adds to the record of fjords as hotspots for carbon preservation (Cui et al., 2016; Smith et al., 2015).

Given the topography of fjords, sediment focusing towards the deepest areas is a common feature in fjords (Noji et al., 1993; Sugai, 1990; Wassmann, 1984; Wiedmann et al., 2015). Burdige (2007) argued that spatial variation together with over representation of muddy sediments might imply that the burial rate in the continental margin might be overestimated for this very reason. In a similar way, overrepresentation of samples at the flat base of fjords might imply that the OC preservation estimates for fjord systems are overestimated. In any case, the large divergence in the obtained carbon burial rate at station T and for the entire fjord (Fig. 7) emphasizes the need to account for spatial variations and sediment focusing when assessing burial efficiencies in complex sea seascapes.

5. Conclusion

The seasonal variation in benthic solute exchange in Kaldbaksfjørður was high considering the stable temperature regime. The dynamics were governed by high primary production and isolated bottom water during summer and intensified sediment resuspension during winter. Lateral advection focused the OC towards the deepest part of the fjord, and in contrast to most systems mineralization increased with

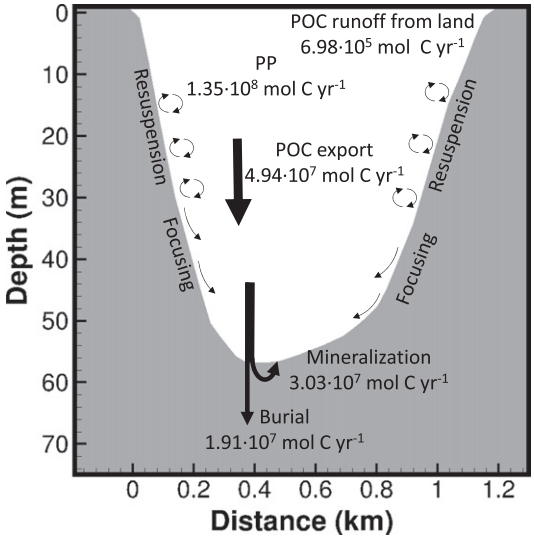

Fig. 7. Annual integrated carbon flow for Kaldbaksfjørður. PP is the primary production during the study period (Gaard et al., 2011). The POC runoff from land is estimated from POC content in riverine water during winter (Table 1) and seasonal freshwater runoff (Gaard et al., 2011). Annual POC export as approximated by the total export from April to September. The approximated annual OC mineralization in the entire fjord taking into account the spatial variation (see this section). The carbon burial is presented as the deposited OC that was unaccounted for in the total OC mineralization.

increasing water depth during summer. The OC burial in the central area of the fjord was 2.4 times higher than averaged over the entire fjord, highlighting the need to account for spatial variations when extrapolating results to entire systems. Taking into account the spatial variations, Kaldbaksfjørður still adds to the record of fjords as important sites for OC burial.

Acknowledgements

This research was supported by Statiol Faroes A/S; Chevron Føroyar Aps.; Geysir Petroleum; the Faroese Research Council [Grant No 0405]; The Danish National Research Council [FNU; 0602-02276B], the European Research Council ERC) under the European Union's Horizon 2020 research and innovation programme [Grant agreement No 669947; HADES-ERC]. We thank personnel at the fish farming company P/F Týggjará, for providing boat and assistance for field measurements, Annie Glud, Southern Danish University, for constructing the applied microelectrodes, and Sólvá Jacobsen, Faroe Marine Research Institute, for her assistance in the laboratory.

References

á Norði, G., Glud, R.N., Gaard, E., Simonsen, K., 2011. Environmental impacts of coastal fish farming: carbon and nitrogen budgets for trout farming in Kaldbaksfjørour (Faroe Islands). Mar. Ecol. Prog. Ser. 431, 223–241. http://dx.doi.org/10.3354/meps09113.

Appleby, P.G., Oldfield, F., 1992. Application of lead-210 to sedimentation studies. In: Ivanovich, M., Harmon, R.S. (Eds.), Uranium-Series Disequlibrium. Applications to Earth, Marine and Environmental Sciences. Clarendon Press, Oxford, pp. 731–778.

Arndt, S., Jørgensen, B.B., LaRowe, D.E., Middelburg, J.J., Pancost, R.D., Regnier, P., 2013. Quantifying the degradation of organic matter in marine sediments: a review and synthesis. Earth-Sci. Rev. http://dx.doi.org/10.1016/j.earscirev.2013.02.008.

Berg, P., Risgaard-Petersen, N., Rysgaard, S., 1998. Interpretation of measured concentration profiles in sediment porewater. Limnol. Oceanogr. 43, 1500–1510.

Bower, C.E., Holm-Hansen, T., 1980. A salicylate–hypochlorite method for determining ammonia in seawater. Can. J. Fish. Aquat. Sci. 37, 794–798. http://dx.doi.org/10.1139/f80-106.

Brenner, H., Braeckman, U., Le Guitton, M., Meysman, F.J.R., 2016. The impact of sedimentary alkalinity release on the water column CO_2 system in the North Sea. Biogeosciences 13, 841–863. http://dx.doi.org/10.5194/bg-13-841-2016.

Buesseler, K.O., Antia, A.N., Chen, M., Fowler, S.W., Gardner, W.D., Gustafsson, O., Harada, K., Michaels, A.F., Rutgers van der Loeff, M., Sarin, M., Steinberg, D.K., Trull, T., 2007. An assessment of the use of sediment traps for estimating upper ocean particle fluxes. J. Mar. Res. 65, 345–416. http://dx.doi.org/10.1357/002224007781567621.

Burdige, D.J., 2007. Preservation of organic matter in marine sediments: controls, mechanisms, and an imbalance in sediment organic carbon budgets? Chem. Rev. 107, 467–485. http://dx.doi.org/10.1021/cr050347q.

Canfield, D.E., 1994. Factors influencing organic carbon preservation in marine sediments. Chem. Geol. 114, 315–329. http://dx.doi.org/10.1016/0009-2541(94)90061-2.

Canfield, D.E., Thamdrup, B., Kristensen, E., 2005. Aquatic geomicrobiology. Advances in Marine Biology 48. Elsevier Academic Press, San Diego.

Carlsson, M., Engström, P., Lindahl, O., Ljungqvist, L., Petersen, J., Svanberg, L., Holmer, M., 2012. Effects of mussel farms on the benthic nitrogen cycle on the Swedish west coast. Aquac. Environ. Interact. 2, 177–191. http://dx.doi.org/10.3354/aei00039.

Cui, X., Bianchi, T.S., Savage, C., Smith, R.W., 2016. Organic carbon burial in fjords: terrestrial versus marine inputs. Earth Planet. Sci. Lett. 451, 41–50. http://dx.doi.org/10.1016/j.epsl.2016.07.003.

Fredriksen, S., 2003. Food web studies in a Norwegian kelp forest based on stable isotope (delta ^{13}C and delta^{15}N) analysis. Mar. Ecol. Prog. Ser. 260, 71–81. http://dx.doi.org/10.3354/meps260071.

Gaard, E., á Norði, G., Simonsen, K., 2011. Environmental effects on phytoplankton production in a Northeast Atlantic fjord, Faroe Islands. J. Plankton Res. 33, 947–959. http://dx.doi.org/10.1093/plankt/fbq156.

Gilbert, R., Nielsen, N., Desloges, J.R., Rasch, M., 1998. Contrasting glacimarine sedimentary environments of two arctic fiords on Disko, West Greenland. Mar. Geol. 147, 63–83. http://dx.doi.org/10.1016/S0025-3227(98)00008-5.

Glud, R.N., 2008. Oxygen dynamics of marine sediments. Mar. Biol. Res. 4, 243–289. http://dx.doi.org/10.1080/17451000801888726.

Glud, R.N., Jensen, K., Revsbech, N.P., 1995. Diffusivity in surficial sediments and benthic mats determined by use of a combined N_2O-O_2 microsensor. Geochim. Cosmochim. Acta 59, 231–237. http://dx.doi.org/10.1016/0016-7037(94)00321-C.

Glud, R.N., Holby, O., Hoffmann, F., Canfield, D.E., 1998. Benthic mineralization and exchange in Arctic sediments (Svalbard, Norway). Mar. Ecol. Prog. Ser. 173, 237–251. http://dx.doi.org/10.3354/meps173237.

Glud, R.N., Gundersen, J.K., Røy, H., Jørgensen, B.B., 2003. Seasonal dynamics of benthic O_2 uptake in a semienclosed bay: importance of diffusion and faunal activity. Limnol. Oceanogr. 48, 1265–1276. http://dx.doi.org/10.4319/lo.2003.48.3.1265.

Glud, R.N., Berg, P., Stahl, H., Hume, A., Larsen, M., Eyre, B.D., Cook, P.L.M., 2016. Benthic carbon mineralization and nutrient turn-over in a Scottish sea loch: an integrative in situ study. Aquat. Geochem. http://dx.doi.org/10.1007/s10498-016-9300-8 (in press).

Grasshoff, K., Kremling, K., Erhardt, M., 1999. Methods of Seawater Analysis. 3rd ed. John Wiley & Sibs, Weinheim.

Gundersen, J.K., Ramsing, N.B., Glud, R.N., 1998. Predicting the signal of O_2 microsensors from physical dimensions, temperature, salinity, and O_2 concentration. Limnol. Oceanogr. 43, 1932–1937. http://dx.doi.org/10.4319/lo.1998.43.8.1932.

Hansen, B., 2011. Veðurlagsbroytingar. Nám, Tórshavn.

Hansen, B., Østerhus, S., 2000. North Atlantic Nordic Seas exchanges. Prog. Oceanogr. 45, 109–208. http://dx.doi.org/10.1016/S0079-6611(99)00052-X.

Jørgensen, B.B., 1996. Material flux in the sediment. Eutrophication Coast. Mar. Ecosyst. 52, pp. 115–135. http://dx.doi.org/10.1029/CE052p0115.

Jørgensen, B.B., Glud, R.N., Holby, O., 2005. Oxygen distribution and bioirrigation in Arctic fjord sediments (Svalbard, Barents Sea). Mar. Ecol. Prog. Ser. 292, 85–95. http://dx.doi.org/10.3354/meps292085.

Kanneworf, E., Nicolaisen, W., 1973. The "HAPS" - a frame supported bottom corer. Ophelia 10, 119–129.

Kristensen, E., 2000. Organic matter diagenesis at the oxic/anoxic interface in coastal marine sediments, with emphasis on the role of burrowing animals. Hydrobiologia 426, 1–24. http://dx.doi.org/10.1023/A:1003980226194.

Lomstein, B.A., Jensen, a.G.U., Hansen, J.W., Andreasen, J.B., Hansen, L.S., Berntsen, J., Kunzendorf, H., 1998. Budgets of sediment nitrogen and carbon cycling in the shallow water of Knebel Vig, Denmark. Aquat. Microb. Ecol. 14, 69–80. http://dx.doi.org/10.3354/ame014069.

Lund-Hansen, L.C., Pejrup, M., Floderus, S., 2004. Pelagic and seabed fluxes of particulate matter and carbon, and C:N ratios resolved by sediment traps during a spring bloom, southwest Kattegat. J. Sea Res. 52, 87–98. http://dx.doi.org/10.1016/j.seares.2003.11.003.

Morata, N., Renaud, P.E., Brugel, S., Hobson, K.a., Johnson, B.J., 2008. Spatial and seasonal variations in the pelagic-benthic coupling of the southeastern Beaufort Sea revealed by sedimentary biomarkers. Mar. Ecol. Prog. Ser. 371, 47–63. http://dx.doi.org/10.3354/meps07677.

Noji, T.T., Noji, C.I.M., Barthel, K.G., 1993. Pelagic-benthic coupling during the onset of winter in a northern Norwegian fjord: carbon flow and fate of suspended particulate matter. Mar. Ecol. Prog. Ser. 93, 89–99.

Porter, E.T., Mason, R.P., Sanford, L.P., 2010. Effect of tidal resuspension on benthic-pelagic coupling in an experimental ecosystem study. Mar. Ecol. Prog. Ser. 413, 33–53. http://dx.doi.org/10.3354/meps08709.

Rasmussen, H., Jorgensen, B.B., 1992. Microelectrode studies of seasonal oxygen uptake in a coastal sediment: role of molecular diffusion. Mar. Ecol. Ser. 81, 289–303. http://dx.doi.org/10.3354/meps081289.

Renaud, P.E., LÃkken, T.S., JÃrgensen, L.L., Berge, J.,, Johnson, B.J., 2015. Macroalgal detritus and food-web subsidies along an Arctic fjord depth-gradient. Front. Mar. Sci. 2, 1–15. http://dx.doi.org/10.3389/fmars.2015.00031.

Revsbech, N.P., 1989. An oxygen microsensor with a guard cathode. Limnol. Oceanogr. 34, 474–478. http://dx.doi.org/10.4319/lo.1989.34.2.0474.

Revsbech, N.P.N., Jørgensen, B.B.B., 1986. Microelectrodes: their use in microbial ecology. Adv. Microb. Ecol. 9, 293–352. http://dx.doi.org/10.1007/978-1-4757-0611-6_7.

Rysgaard, S., Risgaard-Petersen, N., Sloth, N.P., Jensen, K., Nielsen, L.P., 1994. Oxygen regulation of nitrification and denitrification in sediments. Limnol. Oceanogr. 39, 1643–1652. http://dx.doi.org/10.4319/lo.1994.39.7.1643.

Rysgaard, S., Thamdrup, B., Risgaard-Petersen, N., Fossing, H., Berg, P., Christensen, P.B., Dalsgaard, T., 1998. Seasonal carbon and nutrient mineralization in a high-Arctic coastal marine sediment, Young Sound, Northeast Greenland. Mar. Ecol. Prog. Ser. 175, 261–276. http://dx.doi.org/10.3354/meps175261.

Skei, J.M., McKee, B., Sundby, B., 2003. Fjords. In: Black, K.D., Shimmield, G.B. (Eds.), Biogeochemistry of Marine Systems. Blackwell Publishing, Oxford, pp. 65–90.

Smith, R.W., Bianchi, T.S., Allison, M., Savage, C., Galy, V., 2015. High rates of organic carbon burial in fjord sediments globally. Nat. Geosci. 8, 450–453. http://dx.doi.org/10.1038/ngeo2421.

Sørensen, H., Meire, L., Juul-Pedersen, T., de Stigter, H., Meysman, F., Rysgaard, S., Thamdrup, B., Glud, R.N., 2015. Seasonal carbon cycling in a Greenlandic fjord: an integrated pelagic and benthic study. Mar. Ecol. Prog. Ser. 539, 1–17. http://dx.doi.org/10.3354/meps11503.

Sugai, S.F., 1990. Transport and sediment accumulation of ^{210}Pb and ^{137}Cs in 2 Southeast Alaskan fjords. Estuaries 13, 380–392. http://dx.doi.org/10.2307/1351783.

Thamdrup, B., Fossing, H., Jørgensen, B.B., 1994. Manganese, iron and sulfur cycling in a coastal marine sediment, Aarhus bay, Denmark. Geochim. Cosmochim. Acta 58, 5115–5129. http://dx.doi.org/10.1016/0016-7037(94)90298-4.

Therkildsen, M.S., Lomstein, B.A., Lomstein, A.B., 1993. Seasonal variation in net benthic C-mineralization in a shallow estuary. FEMS Microbiol. Ecol. 12, 131–142. http://dx.doi.org/10.1111/j.1574-6941.1993.tb00025.x.

Walinsky, S.E., Prahl, F.G., Mix, A.C., Finney, B.P., Jaeger, J.M., Rosen, G.P., 2009. Distribution and composition of organic matter in surface sediments of coastal Southeast Alaska. Cont. Shelf Res. 29, 1565–1579. http://dx.doi.org/10.1016/j.csr.2009.04.006.

Wassmann, P., 1984. Sedimentation and benthic mineralization of organic detritus in a Norwegian fjord. Mar. Biol. 83, 83–94. http://dx.doi.org/10.1007/BF00393088.

Wiedmann, I., Reigstad, M., Marquardt, M., Vader, A., Gabrielsen, T.M., 2015. Seasonality of vertical flux and sinking particle characteristics in an ice-free high arctic fjord – different from subarctic fjords? J. Mar. Syst. 154, 192–205. http://dx.doi.org/10.1016/j.jmarsys.2015.10.003.

Zajączkowski, M., Szczuciński, W., Bojanowski, R., 2004. Recent changes in sediment accumulation rates in Adventfjorden, Svalbard. Oceanologia 46, 217–231.